Received: 17 October 2020 | Revised: 12 January 2021 | Accepted: 11 April 2021

IET Nanobiotechnology

DOI: 10.1049/nbt2.12054

The Institution of Engineering and Technology WILEY

ORIGINAL RESEARCH PAPER

Antimicrobial potential and *in vitro* cytotoxicity study of polyvinyl pyrollidone-stabilised silver nanoparticles synthesised from *Lysinibacillus boronitolerans*

Divya Bhatia[1] | **Ashwani Mittal**[2] | **Deepak Kumar Malik**[1]

[1]University Institute of Engineering and Technology, Kurukshetra University, Kurukshetra, India

[2]Institute of Integrated and Honors Studies, Kurukshetra University, Kurukshetra, India

Correspondence

Deepak Kumar Malik, University Institute of Engineering and Technology, Kurukshetra University, Kurukshetra, India.
Email: deepmolbio@rediffmail.com

Funding information

University Grants Commission

Abstract

The main emphasis herein is on the eco-friendly synthesis and assessment of the antimicrobial potential of silver nanoparticles (AgNPs) and a cytotoxicity study. Silver nanoparticles were synthesised by an extracellular method using bacterial supernatant. Biosynthesised silver nanoparticles were characterised by UV-vis spectroscopy, transmission electron microscopy (TEM), Fourier transform infrared spectroscopy, dynamic light scattering, and zeta potential analysis. The synthesised silver nanoparticles exhibited a characteristic peak at 420 nm. TEM analysis depicted the spherical shape and approximately 20 nm size of nanoparticles. Silver nanoparticles carry a charge of −33.75 mV, which confirms their stability. Biogenic polyvinyl pyrrolidone-coated AgNPs exhibited significant antimicrobial effects against all opportunistic pathogens (Gram-positive and Gram-negative bacteria, and fungi). Silver nanoparticles equally affect the growth of both Gram-positive and Gram-negative bacteria, with a maximum inhibition zone observed at 22 mm and a minimum at 13 mm against *Pseudomonas aeruginosa* and *Fusarium graminearum*, respectively. The minimum inhibitory concentration (MIC) of AgNPs against *P. aeruginosa* and *Staphylococcus aureus* was recorded at between 15 and 20 μg/ml. Synthesised nanoparticles exhibited a significant synergistic effect in combination with conventional antibiotics. Cytotoxicity estimates using C2C12 skeletal muscle cell line via 3-(4,5-dimethylthiazol-2-yl)-2,5-diphenyltetrazolium bromide (MTT) test and lactate dehydrogenase assay were directly related to the concentration of AgNPs and length of exposure. On the basis of the MTT test, the IC50 of AgNPs for the C2C12 cell line was approximately 5.45 μg/ml concentration after 4 h exposure.

1 | INTRODUCTION

In recent decades, antimicrobial resistance has become a widely recognised and emerging problem worldwide. Excessive use of antibiotics and the emergence of new resistance mechanisms are imposing a challenge to the existing strategies to treat infections. This is a serious call to develop novel products to treat life-threatening infections. To cope with this issue, nanotechnology is emerging as a propitious approach. Over the last few decades, nanotechnology has been rapidly flourishing by producing nanomaterials with novel properties differing significantly from those of the larger particles [1]. Nanoparticles possess unique physiochemical properties owing to their high surface-area-to-volume ratio. The application of metal nanoparticles has revolutionised various areas such as physics, chemistry, material science, and biological science. Among the metal nanoparticles, silver nanoparticles (AgNPs) are the most captivating because of their huge industrial potential [2]. Silver has been regularly used in food and medicine since ancient times, but nanosize silver may have diverse applications. Silver nanoparticles also exhibit improved broad-spectrum antimicrobial activity against various bacterial and fungal pathogens.

Various physical, chemical, and biological methods have been employed for the synthesis of nanoparticles [3–6]. Physical and chemical methods have limitations due to use of toxic chemicals, and high pressure and temperature. There is a serious need for the development of an eco-friendly and economic process for the synthesis of AgNPs. Green nanotechnology, based on the integration of green chemistry and engineering, has significantly contributed to overcoming the limitations associated with existing synthesis processes. Green synthesis methods employ different biological resources such as plants, bacteria, and fungi for the fabrication of nanomaterials. Biological material acts as a reducing agent for the fabrication of nanoparticles [7].

Recently, bacteria-mediated nanomaterial synthesis has been gaining increasing attention due to the easy handling and maintenance. The first bacteria-mediated synthesis was reported in 1984 using *Pseudomonas stutzeri* [8]. Since then, several bacteria and fungi have been explored for silver nanoparticle synthesis. Despite the availability of extensive research related to the biomediated synthesis of nanoparticles, the synthesis of stable, monodispersed nanoparticles with controlled size and shape remains a challenge. Bacterial synthesis of metal nanoparticles can be performed by both intracellular and extracellular methods [9]. The intracellular approach for nanoparticle synthesis is costly and time consuming, as it includes some additional steps for purification of nanoparticles [10]. Therefore, extracellular biosynthesis is favoured over the intracellular method due to the economic and simpler downstream processing requirements.

Recently, AgNPs have been frequently used in catheters [11], wound dressings [12], and the textiles and food industries [13] owing to their efficacy as broad-spectrum antimicrobial agents. Silver nanoparticles exhibit an oligodynamic effect on pathogens owing to their ability to penetrate the cell membrane, bind with biomolecules, and generate free radicals [14]. Despite their broad applications, there is a serious concern about the silver nanoparticle-associated risks to health and the environment. The nanometre size of particles permits their easy entry into the cells of living organisms, leading to cell death [15, 16]. Different factors including particle size, shape, capping agent, agglomeration, type of reducing agents used, and cell type can influence the associated cytotoxicity [17]. However, biosynthesised nanoparticles, being eco-friendly, are less toxic than chemically synthesised ones [11].

Herein, the eco-friendly and cost-effective synthesis of stable nanoparticles in a shorter time is reported, along with the antimicrobial potential of biogenic nanoparticles. To minimise the time and costs of the synthesis process, bacterial cell-free supernatant was used for the synthesis of nanoparticles. This is the first report to test the cytotoxic effect of silver nanoparticles on the muscle cell line. To the best of the authors' knowledge, no study yet has reported testing the cytotoxicity of biogenic silver nanoparticles against a muscle cell line.

2 | MATERIALS AND METHODS

2.1 | Isolation, characterisation, and screening of bacteria for silver nanoparticle synthesis

The isolation of bacteria for silver nanoparticle synthesis was carried out by the serial dilution of soil [18]. Purified bacteria for silver nanoparticle synthesis were identified by BLAST analysis of 16S rRNA sequencing from the Institute of Microbial Technology, Chandigarh (India). A phylogenetic tree was constructed by the neighbour-joining method.

2.2 | Optimisation of extracellular biosynthesis of silver nanoparticles

AgNPs were synthesised using the extracellular method [18]. Bacterial supernatant with 2 mM silver nitrate (in the ratio of 1:1) and polyvinyl pyrrolidone (0.1% PVP) as a stabilising agent, and supernatant with 2 mM silver nitrate (in the ratio of 1:1) without stabilising agent were incubated under bright and dark conditions for 30 min. Supernatant and silver nitrate were also incubated separately under the same conditions. The effect of silver nitrate concentration and incubation time on silver nanoparticle synthesis was observed by UV–visible spectral analysis. The effect of incubation time on silver nanoparticle synthesis was observed at different time intervals (2, 5, 10, 15, 20, and 30 min). The silver nitrate (2 mM) and supernatant were mixed in different ratios, that is 2:3, 1:1, 3:2, 7:3, 4:1, and 9:1, and the final concentrations of silver nitrate were 0.8, 1.0, 1.2, 1.4, 1.6, and 1.8 mM, respectively. Then, the resulting solutions were incubated for an optimum time under bright conditions for the synthesis of AgNPs. The silver nitrate (2 mM) and supernatant were mixed in the optimum ratio and incubated at different temperatures (20, room temperature [under sunlight], 37°C, 40°C, 50°C , and 60°C for the optimum time). The synthesis process of AgNPs was examined visually by observing a change in the colour of the culture supernatant from a clear solution to brown.

2.3 | Characterisation of biologically synthesised silver nanoparticles

The silver nanoparticle synthesis was primarily analysed by UV–visible spectroscopy between 300 and 900 nm (Shimadzu, UV Pharma spec 2550 with a resolution of 0.72 nm). Deionised water was considered as a blank for all experiments. The phase structure and material identification were carried out on the basis of X-ray diffraction (XRD) analysis. The size and morphology of silver nanoparticles were characterised by transmission electron microscopy (TEM) (Hitachi H-750, electron kinetic energy 120 Kv) from CIL, Panjab University, Chandigarh, India. The zeta potential and the size distribution profile of AgNPs were measured using dynamic light scattering (DLS) analysis. Biosynthesised silver nanoparticles were further analysed by fourier transform infrared (FTIR)

spectrophotometry (spectral range of 4000–400 cm^{-1} at a scan speed of 16 cm/s) to identify the functional molecules involved in the reduction of silver nitrate. The elemental distribution of biologically synthesised silver nanoparticles was identified by energy dispersive X-ray spectroscopy (EDX).

2.4 | Analysis of the antimicrobial activity of AgNPs

The antimicrobial effect of biosynthesised silver nanoparticles was evaluated against 10 different test pathogens (seven bacteria and three fungi) by agar well diffusion assay, as reported earlier [18]. The test microorganisms used were *Escherichia coli* (MTCC No. 40), *Bacillus subtilis* (MTCC No. 441), *Pseudomonas aeruginosa* (MTCC No. 424), *Pseudomonas fluorescens* (MTCC No. 1748), *Staphylococcus aureus* (MTCC No. 87), *Streptococcus mutans* (MTCC No. 497), *Streptococcus pyogenes* (MTCC No. 1924), *Fusarium graminearum* (MTCC No. 2089), *Candida albicans* (MTCC No. 3017), and *Candida glabrata* (MTCC No. 3019). The cultures were procured from MTCC, Institute of Microbial Technology, Chandigarh, India. After incubation, a zone of inhibition was measured and recorded as mean ± SD of the triplicate experiment. Different concentrations (19.5, 39, 78.1, 156.2, 312.5, 625, 1250, and 2500 μg) of silver nanoparticles were used to calculate the minimum inhibitory concentration (MIC). The minimum concentration of AgNPs that inhibits the growth of test pathogens was considered as the MIC.

2.5 | The growth curve in the presence of silver nanoparticles

The effect of synthesised silver nanoparticles on bacterial growth (*P. aeruginosa* and *S. aureus*) was analysed in liquid broth by measuring the optical density at a regular interval of 2 h (up to 20 h) at 600 nm. Bacteria were grown in NB medium up to 2 × 108 CFU/ml and further transferred to respective liquid NB media supplemented with 5, 10, 15, 20, 25, and 50 μg/ml of AgNPs. All flasks were incubated at 30°C under shaking conditions (150 rpm). The nutrient broth without silver nanoparticles was used as a control. The interactions between test pathogens (*P. aeruginosa* and *S. aureus*) and biologically synthesised AgNPs were examined by TEM analysis.

2.6 | Synergistic effect of AgNPs with antibiotics

The combined effect of synthesised silver nanoparticles and antibiotics was evaluated by disc diffusion assay. Five different classes of antibiotics, that is (1) quinolone (norfloxacin 10 μg), (2) macrolide (erythromycin 15 μg), (3) rifamycin (rifampicin 5 μg), (4) aminoglycoside (kanamycin 30 μg), and (5) β-lactam (amoxyclav 30 μg) were selected to measure the synergistic effect of silver nanoparticles. Antibiotic discs were impregnated with 30 μl biologically synthesised AgNPs (0.1 mg/ml). The antibiotic discs without silver nanoparticles were considered as a control. The antibiotic discs were placed on nutrient agar plates spread with test pathogens and incubated at 30°C for 24 h. The zone of inhibition was measured and calculated as the mean ± SD of the triplicate experiment. An independent *t*-test analysis was performed to confirm the statistically significant difference between the antimicrobial effect of antibiotics alone and in combination with silver nanoparticles. The level of significance was set at a P-value of <0.05.

2.7 | Cytotoxicity study of silver nanoparticles on the C2C12 skeletal muscle cell line

The cytotoxic effect of silver nanoparticles was evaluated by measuring cell viability, using the 3(4,5-dimethylthiazol2yl)2,5-diphenyltetrazolium bromide (MTT) dye reduction assay and lactate dehydrogenase (LDH) leaking out of the cell. The C2C12 myoblast cells (approximately ~ 30,000/well) were grown in 48-well plates for 24 h in a CO_2 incubator at 5% CO_2 and 37°C. In MTT assay, cells were incubated with different concentrations of silver nanoparticles (0.25, 0.5, 1.0, 2.0, 4.0, 6.0, 8.0, 10.0, 12, and 15 μg/ml) for 4 h and with concentrations (1, 2, 4, 6 and 8 μg/ml) for 24 h. In the LDH assay, the cells were treated with different concentrations (1, 2, 4, 6, and 8 μg/ml) of silver nanoparticles for 4 h. The cells without the treatment of silver nanoparticles were considered as a control. All the experiments were carried out in triplicate. The half MIC (IC50), the concentration required to inhibit the growth of cells by 50%, was measured.

3 | RESULTS

Pure bacterial colonies isolated from soil samples were screened for their ability to grow over nutrient agar plates containing silver nitrate ($AgNO_3$). An isolated bacteria, DNP20, was selected for the extracellular synthesis of silver nanoparticles. The 16S rDNA sequence of DNP20 was analysed by BLAST and the result indicated 100% identity to *Lysinibacillus boronitolerans* (Figure 1). The 16S rDNA sequence of DNP20 was submitted to NCBI with the accession number KU557448.

The flasks containing supernatant of selected bacterial isolates with silver nitrate (2 mM) (with and without PVP) incubated under bright conditions exhibited a colour change from transparent to dark brown. However, the colour change was not observed in the control and flasks incubated under dark conditions even after 5 days

3.1 | Optimisation of the extracellular biosynthesis of silver nanoparticles

The UV–visible spectrum analysis of silver nanoparticles at different time intervals is shown in Figure 2a. The progress

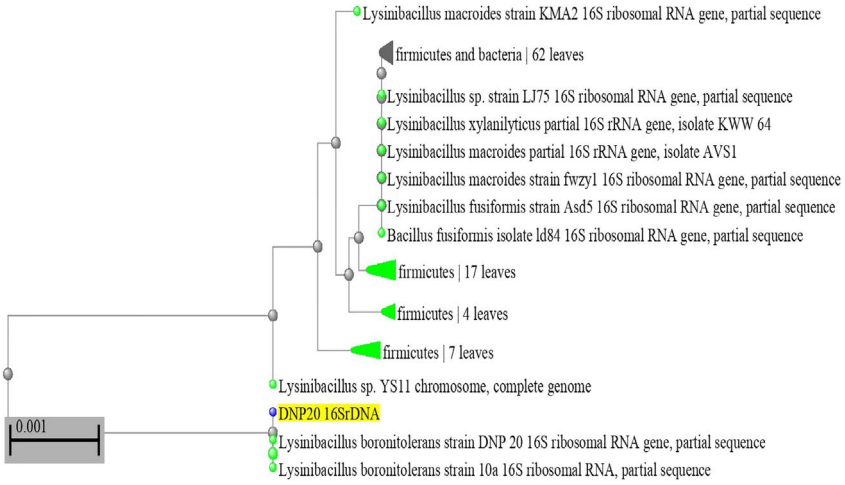

FIGURE 1 Phylogenetic tree constructed by the neighbour joining method

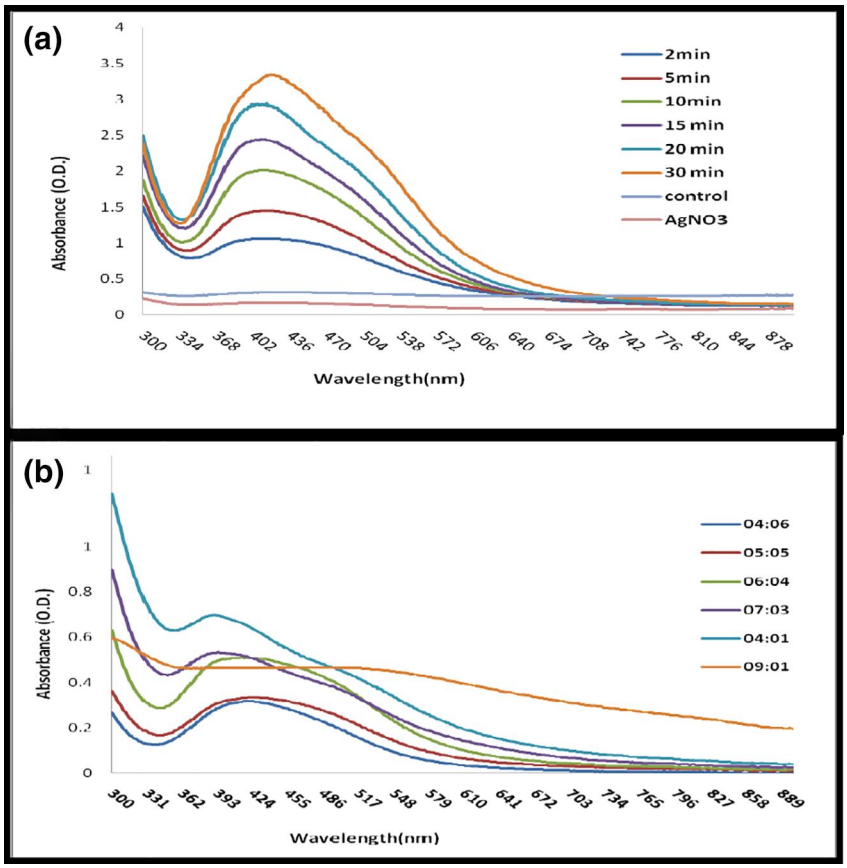

FIGURE 2 UV–visible spectral analysis of silver nanoparticles synthesis: (a) at different time intervals; (b) by using different concentration of silver nitrate

of the reaction was confirmed by monitoring the increment in surface plasmon resonance (SPR) band intensity. Continuation of the reaction was confirmed by monitoring the increment in SPR band intensity. A continued increase in the SPR peak intensity of AgNPs up to 30 min indicates that the reduction of silver ions was in the process, whereas no significant improvement in peak intensity after 30 min denoted the completion of the reduction process. Based on this observation, a 30 min exposure time was fixed for further experiments. A continued increase in SPR peak intensity was observed with an increase in the concentration of silver nitrate up to 1.6 mM, but at a higher concentration of silver nitrate broadening of the peak occurred (Figure 2b). A broad peak depicts large nanoparticles. The SPR peak was not observed in the highest concentration (1.8 mM) of silver nitrate. The observation revealed that a 1 mM concentration was optimum for the synthesis of AgNPs. The incubation temperature exhibited a direct impact on the reduction of silver nitrate into silver nanoparticles. The flasks incubated at room temperature (under sunlight) exhibited a colour change

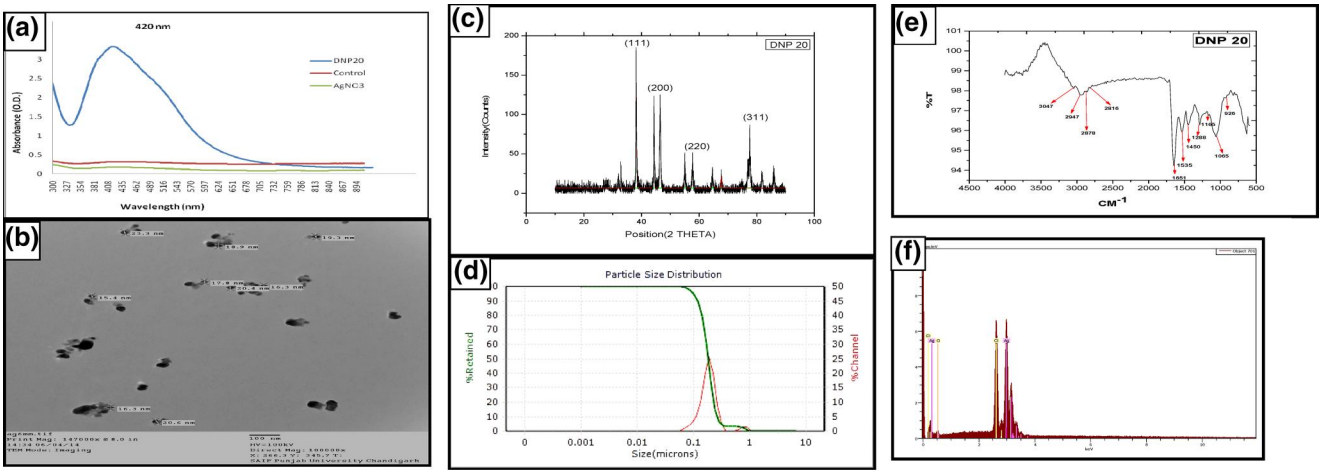

FIGURE 3 (a) UV-visible spectral analysis, (b) TEM analysis, (c) XRD analysis, (d) DLS analysis, (e) FTIR analysis, and (f) EDX analysis of synthesised AgNPs. AgNPs, silver nanoparticles; DLS, dynamic light scattering; EDX, energy dispersive X-ray spectroscopy; FTIR, fourier transform infrared; TEM, transmission electron microscopy; XRD, X-ray diffraction

from transparent to brown within 15 min of incubation. The flasks incubated at 37°C and 40°C exhibited a slight colour change after 24 h. However, the colour change was not observed in flasks incubated at 20°C, 50°C, and 60°C even after 48 h of incubation.

3.2 | Characterisation of silver nanoparticles

UV–visible spectroscopy analysis of AgNPs exhibited a characteristic sharp peak around 420 nm, which confirmed the synthesis of AgNPs (Figure 3a). The absorbance peak position was stable even after 30 days. This confirmed the stability of silver nanoparticles. Based on TEM analysis, silver nanoparticles were spherical, with size ranging from 10 to 30 nm (Figure 3b) and the estimated average size was 20.5 nm (based on 30 particles). In XRD analysis of PVP-coated silver nanoparticles, four diffraction peaks were observed at 2θ values 38.14, 46.46, 64.64, and 77.43, that can be respectively indexed to (111), (200), (220), and (311) planes of pure silver, as shown in Figure 3c. However, silver nanoparticles synthesised without PVP exhibited peaks corresponding to silver oxide. Based on the Debye–Scherer's equation, the average calculated size of silver nanoparticles was 23.24 nm.

Based on DLS analysis, the estimated size of silver nanoparticles was between 130 and 200 nm, carrying a charge of −33.75 mV (Figure 3d). The polydispersity index (PdI) for silver nanoparticles was less than 0.282. Strong peaks at 3047, 2947, 1651 cm^{-1}, 1535, 1288, and 1065 cm^{-1} were observed in the FTIR spectrum of AgNPs (Figure 3e). The EDX analysis revealed a strong signal in the silver region (at 3 keV) because of SPR and confirmed the synthesis of silver nanoparticles (Figure 3f). The EDX spectrum revealed the silver (66.28%), chlorine (18.92%), and oxygen (14.8%), respectively.

3.3 | Antimicrobial activity of biologically synthesised silver nanoparticles against pathogens

The clear zone of inhibition was observed against all test pathogens in the wells containing silver nanoparticles and silver nitrate but not in the wells containing only culture supernatant. The highest antimicrobial activity was observed against *P. aeruginosa* (22 ± 1.32 mm) and the lowest activity was found against *F. graminearum* (13.5 ± 0.5 mm) (Figure 4a). However, silver nanoparticles exhibited significantly higher antimicrobial activity than silver nitrate against *E. coli* (8.82%), *S. aureus* (10%), *S. pyogenes* (16.86%), and *C. albicans* (11.2%). *F. graminearum* was sensitive to AgNPs but resistant to silver nitrate. In the described study, 39 μg concentrations of AgNPs were found to be the MIC for *P. aeruginosa* (15 mm), *S. pyogenes* (15 mm), *F. graminearum* (12 mm), *C. albicans* (11 mm), and *C. glabrata* (15 mm). The MIC for both *E. coli* (14 mm) and *S. aureus* (11 mm) was recorded as 19.5 μg. The MIC for *B. subtilis* was recorded as 78 and 156 μg for *P. fluorescens* (13 mm) and *S. mutans* (15 mm) (Figure 4b).

3.4 | Effect of silver nanoparticles on the bacterial growth curve

In a case of *P. aeruginosa*, normal bacterial growth was observed in a control flask (without silver nanoparticles). At different concentrations of silver nanoparticles (2.5, 5, 10, and 15 μg/ml) the difference in initial growth delay was observed. The delay in growth was proportional to the concentration of AgNPs. However, no growth was observed even after 24 h at higher concentrations (20, 25, and 50 μg/ml) of AgNPs. Therefore, 20 μg/ml may be the MIC of AgNPs against *P. aeruginosa* (Figure 5a). Similarly, with *S. aureus*, normal bacterial growth was observed in a control flask (without silver

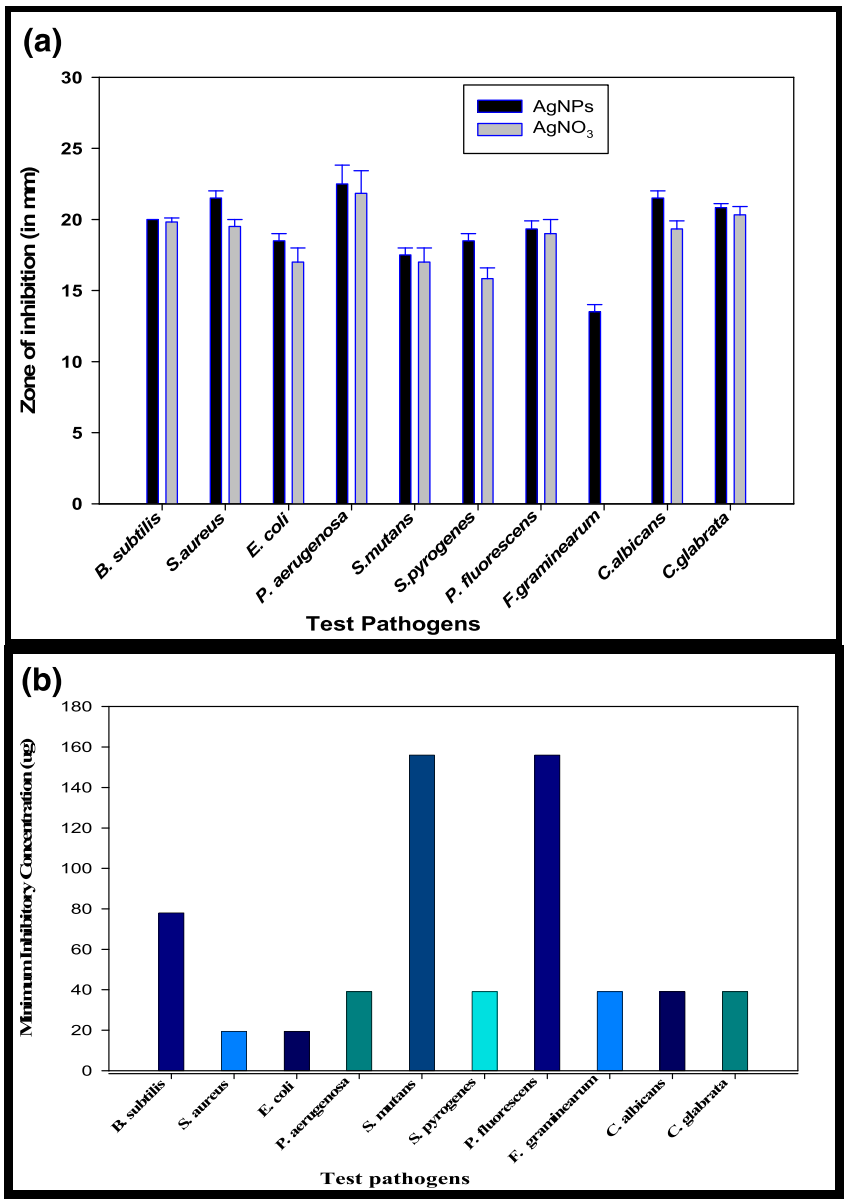

FIGURE 4 (a) Inhibition zone (diameter in mm); (b) minimum inhibitory concentration of silver nanoparticles

nanoparticles). The biologically synthesised AgNPs delayed the growth of *S. aureus* by 1 h when supplemented at a 2.5 μg/ml concentration. The higher concentration (5–10 μg/ml) of silver nanoparticles delayed bacterial growth by 6–7 h. However, no growth was observed even after 24 h, when exposed to a higher concentration (15–50 μg/ml) of silver nanoparticles. The MIC of AgNPs against *S. aureus* can be considered as 15 μg/ml (Figure 5b).

P. aeruginosa cells without silver nanoparticle treatment were of normal morphology with well-developed flagella (Figure 6a). TEM images confirmed the adherence and entry of silver nanoparticles inside the bacterial cells (Figure 6b,c). The untreated *S. aureus* maintained their morphology and appeared to be normal. The electron-dense particles adhered to the cell membrane and morphological changes were observed in cells exposed to silver nanoparticles (Figure 6d). In treated *S. aureus*, cells become constricted in shape and were ruptured after damage to the cell walls.

3.5 | Synergistic effect of AgNPs with antibiotics

The synergistic interaction of AgNPs and norfloxacin was observed against *B. subtilis*, *E. coli*, *P. aeruginosa*, *S. mutans*, *S. pyogenes*, *F. graminearum*, *C. albicans*, and *C. glabrata* (Figure 7a). The highest synergistic effect was detected against *B. subtilis*, however, the synergistic effect was not observed against *S. aureus* and *P. fluorescens*. The synergistic effect of rifampicin and silver nanoparticles was observed against all the test pathogens. A significant synergistic effect was observed against *S. pyogenes*, *P. fluorescens*, *F. graminearum*, *C.*

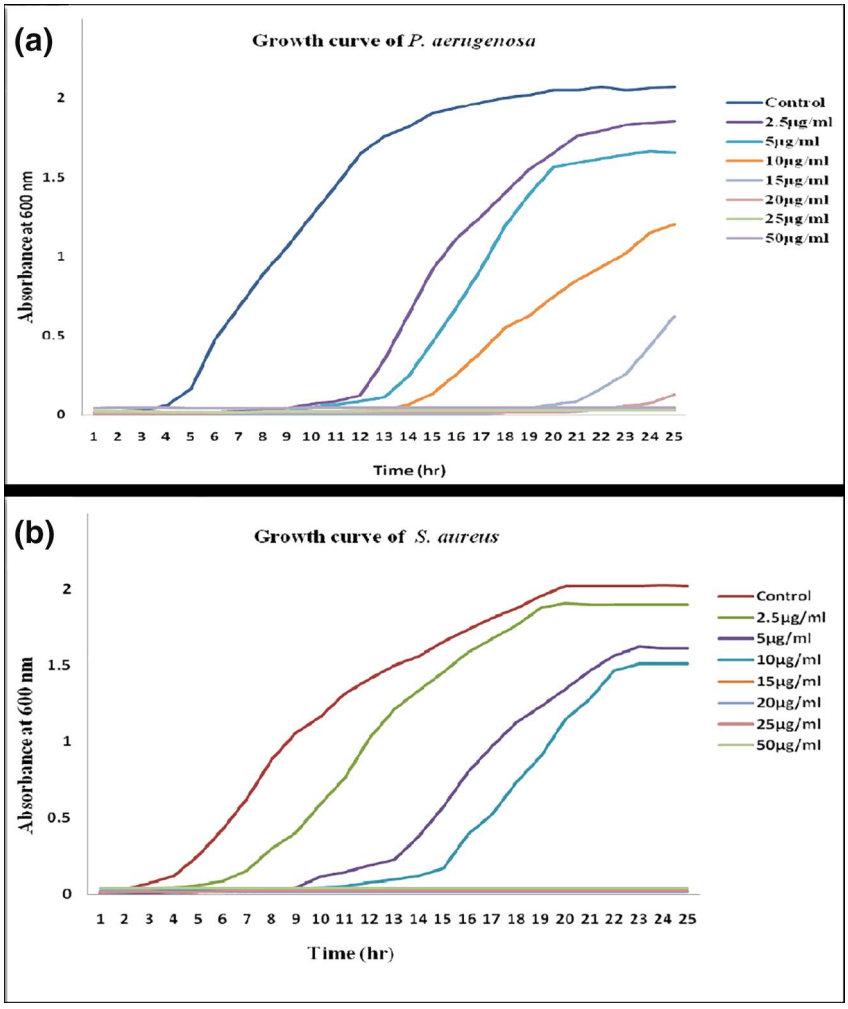

FIGURE 5 Growth curve of Pseudomonas aeruginosa (a) and Staphylococcus aureus (b) treated with different concentrations of silver nanoparticles

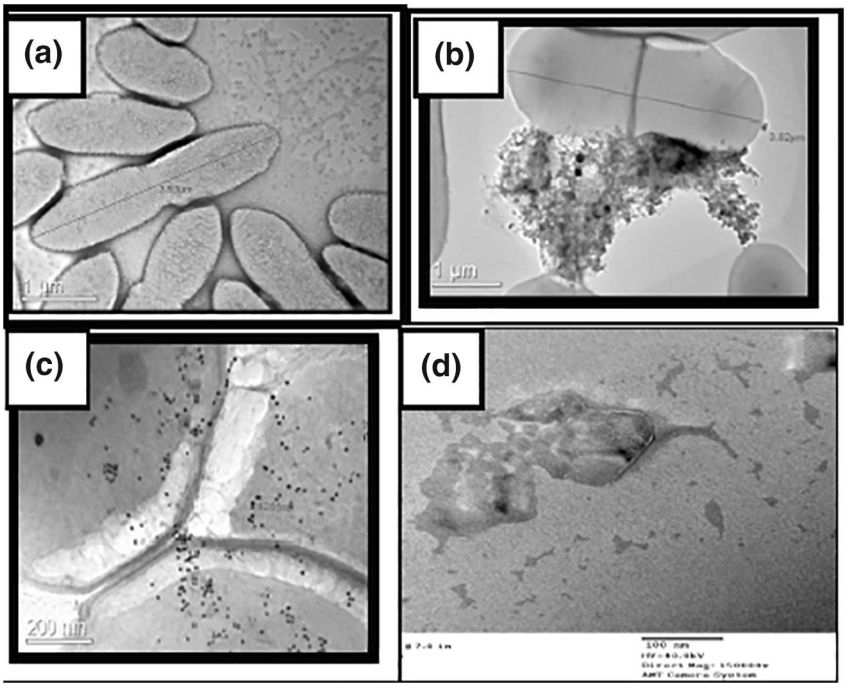

FIGURE 6 Transmission electron microscopy images of (a) Pseudomonas aeruginosa untreated, (b & c) P. aeruginosa treated with 50 µg/ml silver nanoparticles (AgNPs), (d) Staphylococcus aureus treated with 50 µg/ml AgNPs

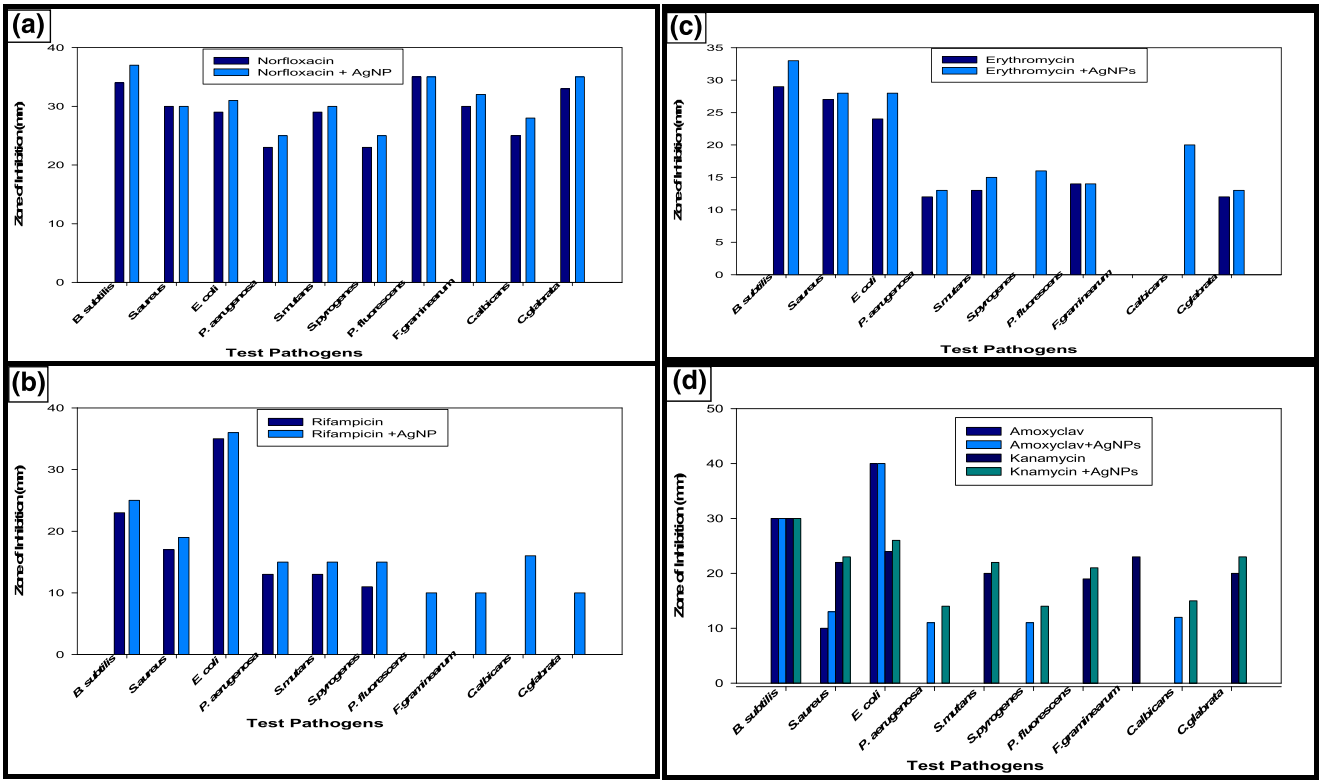

FIGURE 7 Diameter of inhibition zone of: (a) norfloxacin, (b) rifampicin, (c) erythromycin, and (d) kanamycin and amoxyclav. AgNP, silver nanoparticle

albicans, and *C. glabrata*, as shown in Figure 7b. The test pathogens including *P. fluorescens*, *F. graminearum*, *C. albicans*, and *C. glabrata* were resistant to rifampicin in the absence of silver nanoparticles. However, the addition of silver nanoparticles rendered the test strain sensitive to antibiotics. The synergistic effect of erythromycin and AgNPs was observed against *B. subtilis*, *E. coli*, *P. aeruginosa*, *S. mutans*, *S. pyogenes*, *C. albicans*, and *C. glabrata* (Figure 7c). The highest synergistic effect was recorded against *S. pyogenes* followed by *B. subtilis* and *C. albicans*. Erythromycin did not show any activity against *S. pyogenes* and *C. albicans* in the absence of silver nanoparticles. However, no activity was observed against *F. graminearum* even in combination with silver nanoparticles.

The synergistic effect of amoxyclav with silver nanoparticles was observed against *S. aureus*, *P. aeruginosa*, *S. pyogenes*, and *C. albicans*. Amoxyclav did not show any activity against *P. aeruginosa*, *S. pyogenes*, and *C. albicans* in the absence of silver nanoparticles (Figure 7d). The synergistic effect was not observed against *B. subtilis* and *E. coli*. However, *S. mutans*, *P. fluorescens*, *F. graminearum*, and *C. glabrata* were resistant to both amoxyclav and a combination of amoxyclav and silver nanoparticles. The synergistic effect of kanamycin with silver nanoparticles was observed against *E. coli*, *S. aureus*, *P. aeruginosa*, *P. fluorescens*, *S. mutans*, *S. pyogenes*, *C. albicans*, *F. graminearum*, and *C. glabrata*. Kanamycin alone did not show any activity against *P. aeruginosa*, *S. pyogenes*, and *C. albicans* but in combination with AgNPs exhibited inhibitory effects, as shown in Figure 7d. The synergistic effect was not observed against *B. subtilis*. There was a statistically significant difference between the antimicrobial effect of antibiotics alone and in combination with silver nanoparticles. The synergistic effect of silver nanoparticles was statistically significant with all antibiotic classes.

3.6 | Cytotoxicity effect of silver nanoparticles on the C2C12 skeletal muscle cell line

The control cells (without silver nanoparticles treatment) were elongated star-shaped and intact, whereas alterations in cell shape and morphology were observed in cells exposed to the higher concentrations of silver nanoparticles. The low concentrations of AgNPs, that is, 0.25, 0.5, 1.0, and 2.0 μg/ml did not show any effect on the morphology of C2C12 cells, even after 24 h treatment. However, the morphology of cells treated with high concentrations of silver nanoparticles was disturbed. Dead cells with a round-shaped morphology were observed when exposed to higher concentrations (4, 6, 8, 10, 12, and 15 μg/ml) of silver nanoparticles (Figure 8).

The cell cytotoxicity of various concentrations of AgNPs towards C2C12 cells after 4 and 24 h treatment is shown in Figure 9a,b, respectively. The low concentrations (0.25, 0.50, 1.0, and 2.0 μg/ml) of AgNPs do not affect the viability of cells significantly. A continuous increase was observed in percentage cytotoxicity with an increase in the concentration of silver nanoparticles. After 4 h treatment, the IC50 of AgNPs for the

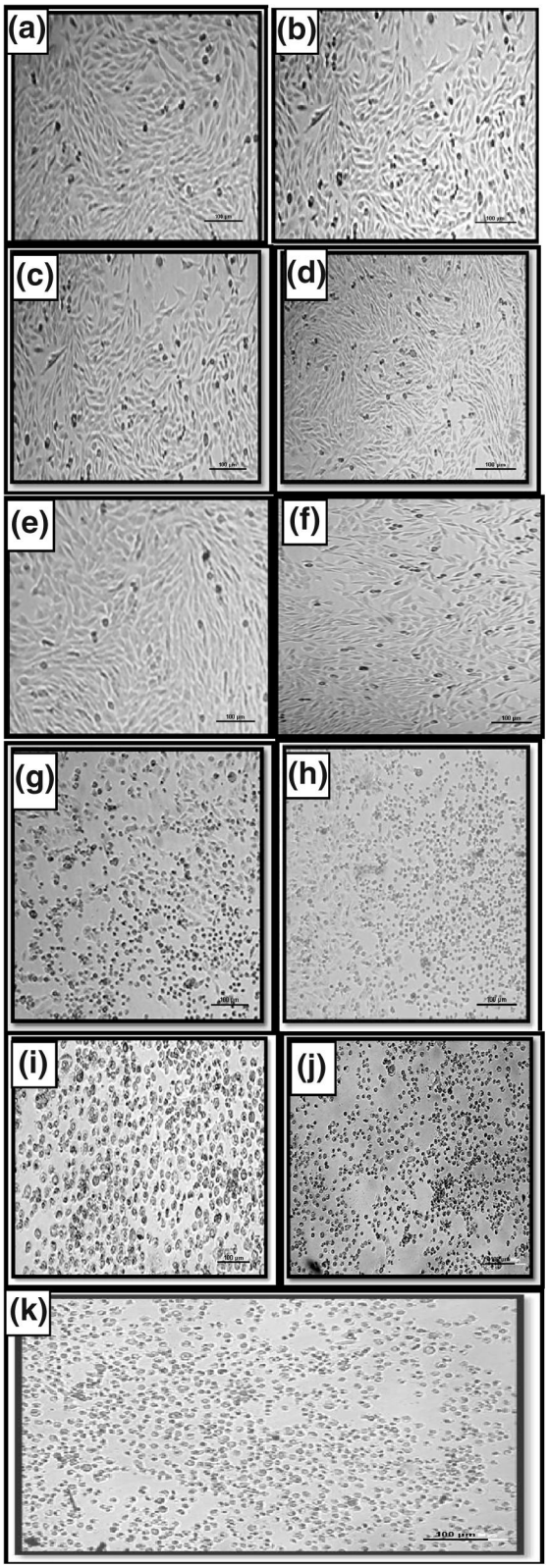

FIGURE 8 Bright field inverted microscopic images of the C2C12 cell line treated with different concentrations of silver nanoparticles (AgNPs) for 4 h: (a) without AgNPs; (b) 0.25 μg/ml; (c) 0.5 μg/ml; (d) 1 μg/ml; (e) 2 μg/ml; (f) 4 μg/ml; (g) 6 μg/ml; (h) 8 μg/ml; (i) 10 μg/ml; (j) 12 μg/ml; (k) 15 μg/ml

C2C12 cell line was estimated at 5.45 μg/ml concentration. The cytotoxicity at a low concentration of silver nanoparticles (1 and 2 μg/ml) was not increased with time of exposure. The exposure of C2C12 cells with high (6 and 8 μg/ml) concentrations of AgNPs for 24 h increased the cytotoxicity to 77% and 96%, respectively. Therefore, it can be inferred that the cytotoxicity of silver nanoparticles is directly related to the silver nanoparticle concentration and length of exposure. LDH assay was used to evaluate the membrane integrity. Significant toxicity in cells treated with higher concentrations (4.0, 6.0 and 8.0 μg/ml) of AgNPs was observed (Figure 9c). When C2C12 cells were treated with 4 μg/ml concentration of silver nanoparticles, approximately 27% of cells were not viable. The exposure of C2C12 cells with 6 and 8 μg/ml concentrations of silver nanoparticles increased the cytotoxicity to 53% and 68%, respectively. It can be inferred that the cell membrane integrity in C2C12 cells was distorted in a dose-dependent manner by biologically synthesised AgNPs. The observed results based on the LDH assay were consistent with the results of the MTT assay.

4 | DISCUSSION

Green synthesis performed at ambient conditions is a relatively easier synthesis process, AND has gained preference over physical and chemical methods [19]. Biogenic synthesis of AgNPs using microorganisms is economical, safe, and eco-friendly [20]. The extracellular method of biosynthesis is favoured over the intracellular method due to the easy and fast purification of nanoparticles. Herein, AgNPs were synthesised extracellularly by DNP 20, identified as *L. boronitolerans*. Other studies have already reported the synthesis of silver nanoparticles by using *Lysinibacillus fusiformis* [21], *Lysinibacillus sphaericus* MR-1 [22], and *Lysinibacillus varians* [18].

A colour change observation is considered as a base for the screening of microbial isolates for silver nanoparticle synthesis [23]. A transition in colour from transparent to a dark-brown colour in the solution confirmed the synthesis of AgNPs. The colour change occurs due to SPR, a characteristic property of silver nanoparticles [24]. Silver nanoparticle synthesis was initiated within 2 min and the process was completed within 30 min. The process adopted here for silver nanoparticle synthesis is much faster than the already reported methods [25]. The effective concentration of $AgNO_3$ is essential for the maximum production of AgNPs. Consistent with the results described here, several other studies have also reported 1 mM concentration of silver nitrate as an optimum concentration [26, 27]. The authors conclude that a slightly high temperature accelerates nanoparticle synthesis. Extracellular synthesis of silver nanoparticles by *Bacillus licheniformis* was carried out at 37°C [28]. However, in another study, a direct relationship between the synthesis of nanoparticles and temperature has been reported [20].

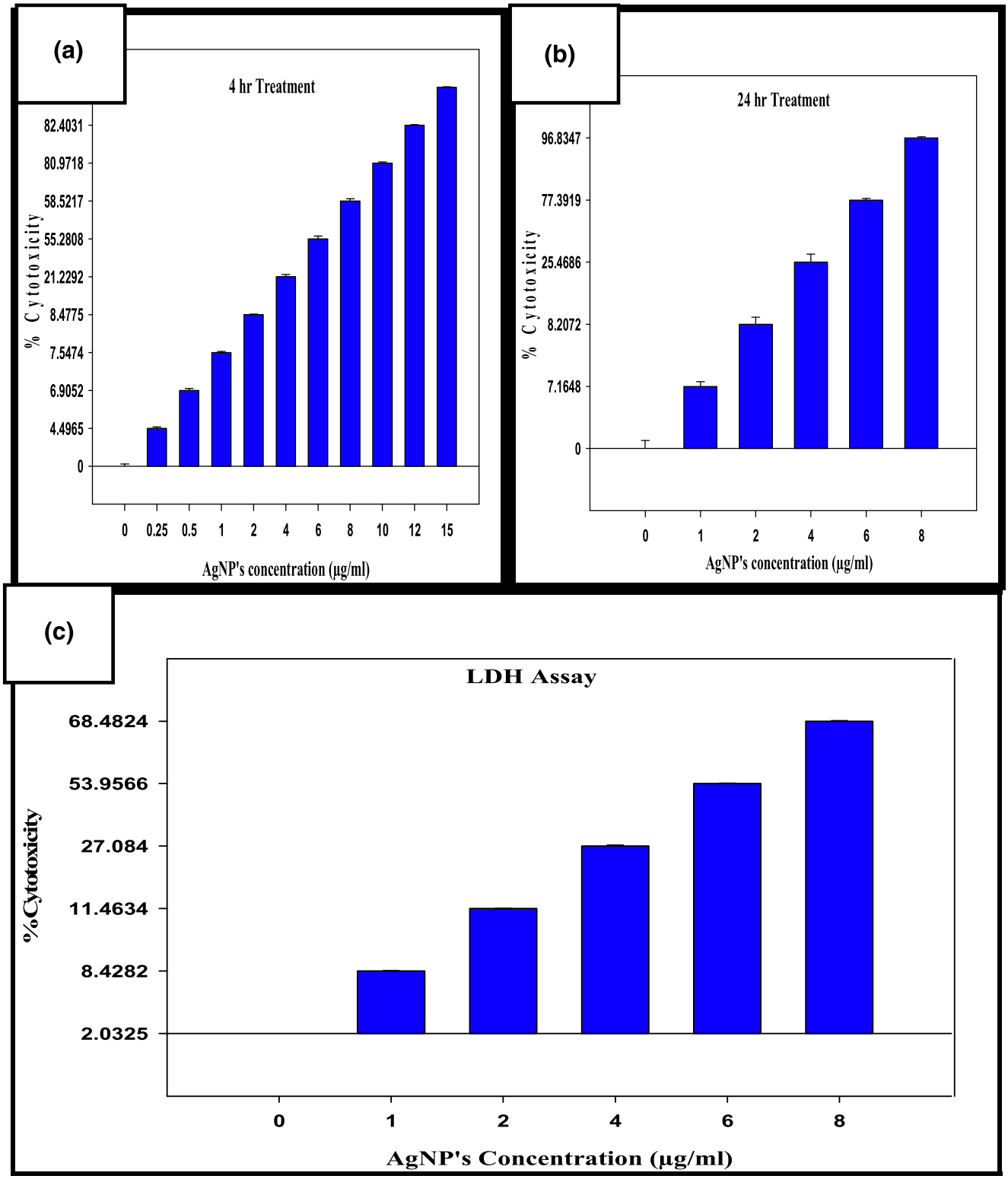

FIGURE 9 Cytotoxicity study of AgNPs synthesised by DNP 20 on C2C12 cells: (a) after 4 h and (b) after 24 h treatment using MTT assay. (c) Cytotoxicity study of AgNPs synthesised by DNP 20 on C2C12 after 4 h treatment using LDH assay. AgNPs, silver nanoparticles; LDH, lactate dehydrogenase; MTT, 3(4,5-dimethylthiazol2yl)2,5-diphenyltetrazolium bromide

In UV–visible spectrophotometric analysis, a sharp peak at 420 nm, that is, the characteristic wavelength for AgNPs, confirmed the synthesis of spherical silver nanoparticles. The UV–vis absorption peak in the visible region (420–450 nm) is due to the SPR phenomenon of AgNPs [29]. The symmetric peak shape with low full width half maximum corresponds to a

narrow size distribution (monodispersity). Spherical nanoparticles exhibit a single characteristic SPR peak, whereas anisotropic molecules show two or more peaks [30]. Particle size, morphology, composition, and dielectric properties of prepared nanoparticles are the key factors that determine the width of SPR bands [31]. The authors observed only one SPR band in UV–visible spectral analysis of synthesised silver nanoparticles and the peak shape was symmetric. Therefore, it can be inferred that synthesised silver nanoparticles were monodisperse and spherical.

The TEM analysis also depicted a spherical shape and nanosize of synthesised particles. The similarity of the observed XRD spectrum with diffraction standard JCPDS 04-0783 confirmed the crystalline nature of synthesised AgNPs. PVP-coated silver nanoparticles were stable, whereas without surfactant, silver-oxide particles were formed. The protective agents used to stabilise metal nanoparticles (NPs) may become attached to nanoparticle surfaces, preventing their aggregation [32]. The size estimated by DLS analysis was larger than that measured by TEM and XRD analysis because DLS analysis not only measures the particle size but also the hydrodynamic size [33]. The PdI below 0.282 and a minimum of ±30 mV charge confirmed the stability of silver nanoparticles [34].

In the FTIR analysis, the peaks present at a position 1651 cm^{-1} correspond to stretching of the C=O amide I band and at 1288 cm^{-1} to stretching of CN amines and NH bending of a peptide. The peak at 926 cm^{-1} was because of aliphatic amines and the peak at 1065 cm^{-1} indicates bending of $–CH_3$ in amino acids. The peaks at 1450 and 1535 cm^{-1} correspond to a change in NO asymmetric stretch due to the nitro compound. The peaks at 2816 and 2878 cm^{-1} indicate C–H stretch in the aldehyde. The peaks at 2947 and 3047 cm^{-1} were observed because of the –CH saturated vibration of saturated hydrocarbons. FTIR peaks of synthesised AgNPs confirmed the role of protein in the synthesis that may attach to nanoparticles via either free NH_2 groups or cysteine residues [35]. Therefore, proteins present in cell-free supernatant may be involved in the reduction and stabilisation of synthesised AgNPs in this process.

In EDX analysis, the presence of a signature signal for silver at 3 keV confirmed the reduction of silver ions to silver element in a reaction mixture [29]. The stable position of an absorbance peak up to 30 days indicated that the silver nanoparticle colloidal solution can remain stable for around 1 month when stored at 4°C. PVP-coated silver nanoparticles were stable for approximately 1 month. However, PVP- and citrate-coated AgNPs are, respectively, reported as the most and least stable NPs in Organisation for Economic Co-operation and Development recommended media (chloride present) [36]. The biogenic AgNPs described herein exhibited significant antimicrobial activity against all tested pathogens (Gram-positive and Gram-negative bacterial strains and fungal strains). The diameter of the inhibition zone increased with an increase in the concentration of silver nanoparticles. The MIC measured here was significantly less than that reported elsewhere. However, the antimicrobial activity depends not only on the silver nanoparticle concentration but varies from species to species depending upon the type of strain, cell wall composition acting as an obstruction to AgNP entry, and microbial sensitivity [21, 37].

The growth curves of bacterial cells exposed to AgNPs revealed inhibition of the growth and reproduction of bacterial cells. As the concentration of silver nanoparticles increased, an increase in lag phase time and a decrease in absorbance were also found in both cases (*P. aeruginosa* and *S. aureus*). At a higher concentration of silver nanoparticles the growth of bacteria was completely inhibited. Similar results were observed for Gram- positive (*S. aureus*) and Gram-negative bacteria (*P. aeruginosa*). Therefore, it can be inferred that silver nanoparticles are equally active against Gram-positive and Gram-negative bacteria. Various other studies have also reported broad-spectrum antibacterial activity of AgNPs against both Gram-negative and Gram-positive bacteria (*E. coli*, *S. aureus*, *B. subtilis*, *S. mutans*, and *Staphylococcus epidermidis*) [38–41]. Thus, the maximum growth delay of bacteria in higher concentrations may be due to excess availability of NPs in the media. The TEM analysis of *P. aeruginosa* and *S. aureus* cells treated cells with AgNPs at 50 µg/ml confirmed the attachment of AgNPs to the cell membrane.

The antimicrobial effect of biosynthesised nanoparticles may be due to the nanosize of particles (9–130 nm). Nanosize particles (size range 10–100 nm) exhibited higher antimicrobial activity than large particles. The exact mechanism involved in antimicrobial activity is not reported, but previous reports suggest that ultrafine particles may cross the cell membrane barrier, encourage the formation of free radicals, damage cell membrane permeability, and damage the respiratory functions of the cell [42, 43]. Strong physical contact between NPs and the bacterial cell wall is crucial for cell damage [39]. The binding of NPs to membrane may disturb the LPS and membrane proteins, leading to a change in the membrane permeability or membrane structure degradation [44–46]. This has been already reported in negatively charged lipopolysaccharides present in Gram-negative bacteria that may attract positively charged AgNPs [47]. However, in herein, the silver nanoparticles synthesised were negatively charged as confirmed by zeta potential measurement. These negatively charged AgNPs may inhibit Gram-negative bacteria by metal reduction [48].

The main reason behind the addition of PVP was to provide stability to the silver nanoparticles. However, it has been already reported that PVP-coated silver nanoparticles are more effective than citrate or SDS-capped nanoparticles owing to the steric stabilisation of nanoparticles by PVP. PVP-capped silver nanoparticles are even stable with changes in pH and ionic strength [49, 50].

The formation of larger zones of inhibition confirmed that antibiotics, when combined with biosynthesised AgNPs, exhibit an enhanced antimicrobial effect against test pathogens. The synergistic effect was statistically significant at the 5% level. Nanoparticles may enable cell wall penetration by the antibiotic to execute an antimicrobial effect. Several other studies have also reported that the amalgamation of silver nanoparticles with different antibiotics leads to a stronger

effect of antibiotics against various microorganisms [51, 52]. Depending on the class of antibiotic used, different levels of activity increments were observed [21]. Nanoparticle antibiotic conjugates may lower the amount of both drugs and nanoparticles needed, and may lead to reduced side effects of medicines while increasing their efficacy [53].

The MTT assay measures cell viability through the increased metabolisation of a tetrazolium salt [54] and LDH assay quantifies the amount of released LDH and measures membrane damage by cytoplasm [55]. Herein, silver nanoparticles at the lower concentration did not show any cytotoxic effect and the viability, as well as morphology of target cells, was at the same level as in the control. However, at higher concentrations, cytotoxicity and altered morphology were observed, proportional to the concentration of AgNPs and time of exposure. In LDH assay, a higher concentration of AgNPs leads to increased leakage of LDH in medium and more cytotoxicity. It has been already reported that AgNP exposure could affect the cell shape, cell viability, and lactate dehydrogenase (LDH) release, and may lead to cell apoptosis and necrosis [56, 57]. It can be inferred from both MTT and LDH assay that silver nanoparticles reduce the cell viability of C2C12 cells in a dose- and time-dependent manner. The cytotoxicity of AgNPs on different cell lines such as human (0.5–3 μg/ml) and rat (10–50 μg/ml) liver cells, alveolar macrophages (10–75 μg/ml), mice dermal fibroblasts and liver cells (30 μg/ml), or mouse germline stem cells (10 μg/ml) has been reported [17, 42, 58–60]. Various studies have already reported that cell viability was directly affected by culture time as well as the AgNP concentration [61, 62].

It has been already reported that 5 nm size AgNPs were more toxic than 20 and 50 nm particles in different cell lines (A549, HepG2, MCF-7, and CGC-7901) [63]. Ultrafine particles, due to their nanosize, exhibit higher activity because of the availability of a larger surface area for interaction [64]. However, in contrast, another study reported that the cells were less viable when exposed to 100-nm AgNPs when compared with small-sized nanoparticles [65]. Surfactant-capped nanoparticles exhibited more damage to mammalian cells than uncapped silver nanoparticles [62]. The size of PVP-capped AgNPs is inversely related to the cell viability [43]. Small AgNPs induced higher toxicity than larger particles (110 nm) [66]. With a few exceptions, capped silver nanoparticles exhibited less cytotoxicity against human cell lines compared to mouse cell lines [67].

The accurate cause of cytotoxicity is not known, but some reports have revealed that silver may interfere with the electron transfer chain [68], produce free radicals [69], or cause ATP leaking [70]. Silver nanoparticles have been reported to disturb mitochondrial processes and enhance membrane seepage and result in oxidative stress [58]. However, the extent of cytotoxicity depends on the size of the AgNPs because AgNP size may affect their penetration through cell membranes [71]. It can be inferred that particle size, morphology nanoparticles, surface coating, culture time, and cell type are the major contributing factors for the variations in cytotoxicity.

5 | CONCLUSION

Herein, the process adopted for the formation of PVP-coated silver nanoparticles was very rapid, economical, and eco-friendly, and can be used as an efficient method for the synthesis of nanoparticles. Silver nanoparticles exhibited broad-spectrum antimicrobial activity and a synergistic effect in combination with existing antibiotics. Therefore, it can be concluded that biogenic AgNPs can be used as a potent antimicrobial agent in various applications. However, prior to their application in the pharmaceutical industry, it is imperative to explain completely the action mechanism of the biosynthesised nanoparticles. PVP-coated silver nanoparticles exhibited cytotoxicity against the C2C12 cell line. However, the cytotoxicity of silver nanoparticles was evaluated only under *in vitro* conditions against a single cell line. A detailed *in vivo* study must be carried out before the commercial use of silver nanoparticles. Further, silver nanoparticles can be modified to increase the antimicrobial efficacy and to decrease the cytotoxic effect.

ACKNOWLEDGEMENTS

The work was financially supported under the scheme of UGC JRF (Ref No. 22/12/2013(ii) EU-V) by the University Grants Commission New Delhi, India to the first author. The authors also thank IMTECH, Chandigarh, India, for bacterial identification and the Sophisticated Analytical Instrument Facility (SAIF), Panjab University, Chandigarh, India, for access to the TEM facility.

ORCID

Divya Bhatia https://orcid.org/0000-0002-1038-6686

REFERENCES

1. Yon, J.N., Jamie, R.L.: Manufactured nanoparticles: an overview of their chemistry, interactions and potential environmental implications. Sci. Total Environ. 400, 396–414 (2008)
2. Elemike, E.E., et al.: Phytosynthesis of silver nanoparticles using aqueous leaf extracts of Lippia citriodora : antimicrobial, larvicidal and photocatalytic evaluations. Mater. Sci. Eng. C. 75, 980–989 (2017)
3. Jorge de Souza, T.A., Rosa Souza, L.R., Franchi, L.P.: Silver nanoparticles: an integrated view of green synthesis methods, transformation in the environment, and toxicity. Ecotoxicol. Environ. Saf. 171, 691–700 (2019)
4. De Matteis, V., et al.: Silver nanoparticles: synthetic routes, in Vitro toxicity and theranostic Applications for cancer disease. Nanomaterials. 8, 319 (2018). https://doi.org/10.3390/nano8050319
5. Jalal, M., et al.: Anticandidal activity of biosynthesised silver nanoparticles: effect on growth, cell morphology, and key virulence attributes of Candida species. Int. J. Nanomed. 14, 4667–4679 (2019)
6. Nakamura, S., et al.: Synthesis and application of silver nanoparticles (Ag NPs) for the prevention of infection in healthcare workers. Int. J. Mol. Sci. 20, 3620–3638 (2019). https://www.ncbi.nlm.nih.gov/pmc/articles/PMC6695748
7. Anand, K.K.H., Mandal, B.K.: Activity study of biogenic spherical silver nanoparticles towards microbes and oxidants. Spectrochim. Acta Mol. Biomol. Spectrosc. 135, 639–645 (2015)
8. Haefeli, C., Franklin, C., Hardy, K.: Plasmid-determined silver resistance in Pseudomonas stutzeri isolated from a silver mine. J Bacteriol. 158, 389–392 (1984)

9. Kalishwaralal, K., et al.: Biosynthesis of silver and gold nanoparticles using Brevibacterium casei. Colloids Surf. B Biointerfaces. 77, 257–262 (2010)
10. Ganesh Babu, M.M., Gunasekaran, P.: Production and structural characterisation of crystalline silver nanoparticles from Bacillus cereus isolate. Colloids Surf. B Biointerfaces. 74, 191–195 (2009)
11. Samuel, U., Guggenbichler, J.P.: Prevention of catheter-related infections: the potential of a new nano-silver impregnated catheter. Int. J. Antimicrob. Agents. 23, 75–78 (2004). https://doi.org/10.1016/j.ijantimicag.2003.12.004
12. Chen, J., et al.: Effect of silver nanoparticle dressing on second degree burn wound. Zhonghua Wai Ke Za Zhi. 44, 50–52 (2006)
13. Vigneshwaran, N., et al.: Functional finishing of cotton fabrics using silver nanoparticles. J. Nanosci. Nanotechnol. 7, 1893–1897 (2007)
14. Prasher, P., Singh, M., Mudila, H.: Oligodynamic effect of silver nanoparticles: a review. BioNanoScience. 8, 951–962 (2018)
15. Greulich, C., et al.: Uptake and intracellular distribution of silver nanoparticles in human mesenchymal stem cells. Acta Biomater. 7, 347–354 (2011). https://doi.org/10.1016/j.actbio.2010.08.003
16. Liz, R., et al.: Silver nanoparticles rapidly induce atypical human neutrophil cell death by a process involving inflammatory caspases and reactive oxygen species and induce neutrophil extracellular traps release upon cell adhesion. Int. Immunopharm. 28, 616–625 (2015). https://doi.org/10.1016/j.intimp.2015.06.030
17. Carlson, C., et al.: Unique cellular interaction of silver nanoparticles: size-dependent generation of reactive oxygen species. J. Phys. Chem. B. 112, 13608–13619 (2008). https://doi.org/10.1021/jp712087m
18. Bhatia, D., Mittal, A., Malik, D.K.: Antimicrobial activity of PVP coated silver nanoparticles synthesised by Lysinibacillus varians. 3 Biotech. 6, 1–8 (2016). https://doi.org/10.1007/s13205-016-0514-7
19. Yousef, N.M.H.: Characterisation and antimicrobial activity of silver nanoparticles synthesised by rice straw utilising bacterium Lysinibacillus fusiformis. Int. J. Dev. Res. 4, 1875–1879 (2014)
20. Gou, Y., et al.: Highly efficientin vitrobiosynthesis of silver nanoparticles usingLysinibacillus sphaericusMR-1 and their characterisation. Sci. Technol. Adv. Mater. 16, 015004–6996 (2015). https://doi.org/10.1088/1468-6996/16/1/015004
21. Singh, R., et al.: Synthesis, optimization and characterisation of silver nanoparticles from Acinetobacter calcoaceticus and their enhanced antibacterial activity when combined with antibiotics. Int. J. Nanomed. 8, 4277–4290 (2013). https://doi.org/10.2147/IJN.S48913
22. Shedbalkar, U., et al.: Microbial synthesis of gold nanoparticles: current status and future prospects. Adv. Colloid Interface Sci. 209, 40–48 (2014). https://doi.org/10.1016/j.cis.2013.12.011
23. Saravanan, M., Vemu, A.K., Barik, S.K.: Rapid biosynthesis of silver nanoparticles from Bacillus megaterium (NCIM 2326) and their antibacterial activity on multi drug resistant clinical pathogens. Colloids Surf. B Biointerfaces. 88, 325–331 (2011). https://doi.org/10.1016/j.colsurfb.2011.07.009
24. Iqbal, E., Salim, K.A., Lim, L.B.L.: Phytochemical screening, total phenolics and antioxidant activities of bark and leaf extracts of Goniothalamus velutinus (Airy Shaw) from Brunei Darussalam. J. King Saud Univ. Sci. 27(3), 224–232 (2015)
25. Vivekanandhan, S., et al.: Maple leaf (Acer sp.) extract mediated green process for the functionalisation of ZnO powders with silver nanoparticles. Colloids Surf. B Biointerfaces. 113, 169–175 (2014). https://doi.org/10.1016/j.colsurfb.2013.08.033
26. Baker, S., Shreedharmurthy, S.: Antimicrobial activity and biosynthesis of nanoparticles by endophytic bacterium inhabiting Coffee arabica L. Sci. J. Biol. Sci. 1, 107–113 (2012)
27. Narayanan, K.B., Sakthivel, N.: Biosynthesis of silver nanoparticles by phytopathogen Xanthomonas oryzae pv. oryzae strain BXO8. J. Microbiol. Biotechnol. 23, 1287–1292 (2013)
28. Kalishwaralal, K., et al.: Extracellular biosynthesis of silver nanoparticles by the culture supernatant of Bacillus licheniformis. Mater. Lett. 62, 4411–4413 (2008). https://doi.org/10.1016/j.matlet.2008.06.051
29. Muthukrishnan, S., et al.: Biosynthesis, characterisation and antibacterial effect of plant-mediated silver nanoparticles using Ceropegiav thwaitesii - an endemic species. Ind. Crop Prod. 63, 119–124 (2015). https://doi.org/10.1016/j.indcrop.2014.10.022
30. Krishnaraj, C., et al.: Synthesis of silver nanoparticles using Acalypha indica leaf extracts and its antibacterial activity against water borne pathogens. Colloids Surf. B Biointerfaces. 76, 50–56 (2010). https://doi.org/10.1016/j.colsurfb.2009.10.008
31. Kelly, K.L., et al.: The optical properties of metal nanoparticles: the influence of size, shape, and dielectric environment. J. Phys. Chem. B. 107, 668–677 (2003). https://doi.org/10.1021/jp026731y
32. Oliveira, M.M., et al.: Influence of synthetic parameters on the size, structure, and stability of dodecanethiol-stabilised silver nanoparticles. J. Colloid Interface Sci. 292, 429–435 (2005). https://doi.org/10.1016/j.jcis.2005.05.068
33. Bhakya, S., et al.: Biogenic synthesis of silver nanoparticles and their antioxidant and antibacterial activity. Appl. Nanosci. 6, 755–766 (2016). https://doi.org/10.1007/s13204-015-0473-z
34. Shah, A., et al.: Daphne mucronata-mediated phytosynthesis of silver nanoparticles and their novel biological applications, compatibility and toxicity studies. Green Chem. Lett. Rev. 11(3), 318–333 (2018)
35. Mandal, S., Phadtare, S., Sastry, M.: Interfacing biology with nanoparticles. Curr. Appl. Phys. 5, 118–127 (2005). https://doi.org/10.1016/j.cap.2004.06.006
36. Tejamaya, M., et al.: Stability of citrate, PVP, and PEG coated silver nanoparticles in ecotoxicology media. Environ. Sci. Technol. 46, 7011–7017 (2012). https://doi.org/10.1021/es2038596
37. Abdeen, S., et al.: Biosynthesis of silver nanoparticles from actinomycetes for therapeutic applications. Int. J. Nano Dimens. (IJND). 5, 155–162 (2014). https://doi.org/10.7508/IJND.2014.02.008
38. Lee, B.U., et al.: Inactivation of S. epidermidis, B. subtilis and E. coli bacteria bioaerosols deposited on a filter utilising airborne silver nanoparticles. J. Microbiol. Biotechnol. 18, 176–182 (2008)
39. Jung, W.K., et al.: Antibacterial activity and mechanism of action of the silver ion in Staphylococcus aureus and Escherichia coli. Appl. Environ. Microbiol. 74, 2171–2178 (2008). https://doi.org/10.1128/AEM.02001-07
40. Karmali, M.A.: Factors in the emergence of serious human infections associated with highly pathogenic strains of shiga toxin-producing Escherichia coli. Int. J. Med. Microbiol. 308(8), 1067–1072 (2018)
41. Espinosa-Cristóbal, L.F., et al.: Antibacterial effect of silver nanoparticles against Streptococcus mutans. Mater. Lett. 63, 2603–2606 (2009). https://doi.org/10.1016/j.matlet.2009.09.018
42. Shankar, S., Rhim, J.-W.: Amino acid mediated synthesis of silver nanoparticles and preparation of antimicrobial agar/silver nanoparticles composite films. Carbohydr. Polym. 130, 353–363 (2015)
43. Li, L., et al.: Controllable synthesis of monodispersed silver nanoparticles as standards for quantitative assessment of their cytotoxicity. Biomaterials. 33, 1714–1721 (2012). https://doi.org/10.1016/j.biomaterials.2011.11.030
44. El Badawy, A.M., et al.: Surface charge-dependent toxicity of silver nanoparticles. Environ. Sci. Technol. 45, 283–287 (2011). https://doi.org/10.1021/es1034188
45. Parashar, U.K., et al.: Study of mechanism of enhanced antibacterial activity by green synthesis of silver nanoparticles. Nanotechnology. 22, 415104–415116 (2011). https://doi.org/10.1088/0957-4484/22/41/415104
46. Selvakumar, R., et al.: A facile synthesis of silver nanoparticle with SERS and antimicrobial activity using Bacillus subtilis exopolysaccharides. J. Exp. Nanosci. 9(10), 1075–1087 (2013). https://doi.org/10.1080/17458080.2013.778425
47. Sui, Z.M., et al.: Capping effect of CTAB on positively charged Ag nanoparticles. Phys E Low-dimens Syst Nanostruct. 33, 308–314 (2006). https://doi.org/10.1016/j.physe.2006.03.151
48. Amro, N.A., et al.: High-resolution atomic force microscopy studies of theEscherichiacoliOuter membrane: structural basis for permeability. Langmuir. 16, 2789–2796 (2000). https://doi.org/10.1021/la991013x
49. Badawy, A.M.E., et al.: Impact of environmental conditions (pH, ionic strength, and electrolyte type) on the surface charge and aggregation of

silver nanoparticles suspensions. Environ. Sci. Technol. 44, 1260–1266 (2010)
50. Hitchman, A., et al.: The effect of environmentally relevant conditions on PVP stabilised gold nanoparticles. Chemosphere. 90, 410–416 (2013)
51. Naqvi, S.Z., et al.: Combined efficacy of biologically synthesised silver nanoparticles and different antibiotics against multidrug-resistant bacteria. Int. J. Nanomed. 8, 3187–3195 (2013). https://doi.org/10.2147/IJN.S49284
52. Singh, P., et al.: Biosynthesis, characterisation and antimicrobial applications of silver nanoparticles. Int. J. Nanomed. 10, 2567–2577 (2015). https://doi.org/10.2147/IJN.S72313
53. Fayaz, A.M., et al.: Biogenic synthesis of silver nanoparticles and their synergistic effect with antibiotics: a study against gram-positive and gram-negative bacteria. Nanomed. Nanotechnol. Biol. Med. 6, 103–109 (2010). https://doi.org/10.1016/j.nano.2009.04.006
54. Moshmann, A.T.: Rapid colourimetric assay for cellular growth and survival: application to proliferation and cytotoxicity assays. J. Immunol. Method. 65, 55–63 (1983). https://doi.org/10.1016/0022-1759(83)90303-4
55. Krysko, D.V., et al.: Apoptosis and necrosis: detection, discrimination and phagocytosis. Methods. 44, 205–221 (2008). https://doi.org/10.1016/j.ymeth.2007.12.001
56. Chen, X., Schluesener, H.J.: Nanosilver: a nanoproduct in medical application. Toxicol. Lett. 176, 1–12 (2008). https://doi.org/10.1016/j.toxlet.2007.10.004
57. Foldbjerg, R., et al.: PVP-coated silver nanoparticles and silver ions induce reactive oxygen species, apoptosis and necrosis in THP-1 monocytes. Toxicol. Lett. 190, 156–162 (2009). https://doi.org/10.1016/j.toxlet.2009.07.009
58. Hussain, S.M., et al.: In vitro toxicity of nanoparticles in BRL 3A rat liver cells. Toxicol. Vitro. 19, 975–983 (2005). https://doi.org/10.1016/j.tiv.2005.06.034
59. Arora, S., et al.: Interactions of silver nanoparticles with primary mouse fibroblasts and liver cells. Toxicol. Appl. Pharmacol. 236, 310–318 (2009). https://doi.org/10.1016/j.taap.2009.02.020
60. Kim, S., et al.: Oxidative stress-dependent toxicity of silver nanoparticles in human hepatoma cells. Toxicol. Vitro. 23, 1076–1084 (2009). https://doi.org/10.1016/j.tiv.2009.06.001
61. AshaRani, P.V., et al.: Cytotoxicity and genotoxicity of silver nanoparticles in human cells. ACS Nano. 3, 279–290 (2009). https://doi.org/10.1021/nn800596w
62. Ahamed, M., et al.: DNA damage response to different surface chemistry of silver nanoparticles in mammalian cells. Toxicol. Appl. Pharmacol. 233, 404–410 (2008)
63. Vazquez-Muñoz, R., et al.: Toxicity of silver nanoparticles in biological systems: does the complexity of biological systems matter? Toxicol. Lett. 276, 11–20 (2017). https://doi.org/10.1016/j.toxlet.2017.05.007
64. He, W., et al.: Mechanisms of the pH dependent generation of hydroxyl radicals and oxygen induced by Ag nanoparticles. Biomaterials. 33, 7547–7555 (2012). https://doi.org/10.1016/j.biomaterials.2012.06.076
65. Kim, S., Ryu, D.-Y.: Silver nanoparticle-induced oxidative stress, genotoxicity and apoptosis in cultured cells and animal tissues. J. Appl. Toxicol. 33, 78–89 (2013). https://doi.org/10.1002/jat.2792
66. Wang, X., et al.: Use of coated silver nanoparticles to understand the relationship of particle dissolution and bioavailability to cell and lung toxicological potential. Small. 10, 385–398 (2013). https://doi.org/10.1002/smll.201301597
67. de Lima, R., Seabra, A.B., Duran, N.: Silver nanoparticles: a brief review of cytotoxicity and genotoxicity of chemically and biogenically synthesised nanoparticles. J. Appl. Toxicol. 32, 867–879 (2012). https://doi.org/10.1002/jat.2780
68. Sharma, V.K., Yngard, R.A., Lin, Y.: Silver nanoparticles: green synthesis and their antimicrobial activities. Adv. Colloid Interface Sci. 145, 83–96 (2009). https://doi.org/10.1016/j.cis.2008.09.002
69. Majeed, S., et al.: Biosynthesis and characterisation of silver nanoparticles from fungal species and its antibacterial and anticancer effect. Karbala Int. J. Mod. Sci. 4, 86–92 (2018). https://doi.org/10.1016/j.kijoms.2017.11.002
70. Kora, A.J., Sashidhar, R.B.: Biogenic silver nanoparticles synthesised with rhamnogalacturonan gum: antibacterial activity, cytotoxicity and its mode of action. Arabian J. Chem. 11, 313–323 (2018). https://doi.org/10.1016/j.arabjc.2014.10.036
71. He, D., Bligh, M.W., Waite, T.D.: Effects of aggregate structure on the dissolution kinetics of citrate-stabilised silver nanoparticles. Environ. Sci. Technol. 47, 9148–9156 (2013). https://doi.org/10.1021/es400391a

How to cite this article: Bhatia D, Mittal A, Malik DK. Antimicrobial potential and *in vitro* cytotoxicity study of polyvinyl pyrollidone-stabilised silver nanoparticles synthesised from *Lysinibacillus boronitolerans*. *IET Nanobiotechnology*. 2021;15:427–440. https://doi.org/10.1049/nbt2.12054